Fresenius J Anal Chem (2001) 371:307–316
DOI 10.1007/s002160100989

TECHNICAL NOTE

H. Bronk · S. Röhrs · A. Bjeoumikhov · N. Langhoff
J. Schmalz · R. Wedell · H.-E. Gorny · A. Herold
U. Waldschläger

ArtTAX – a new mobile spectrometer for energy-dispersive micro X-ray fluorescence spectrometry on art and archaeological objects

Received: 12 April 2001 / Revised: 6 June 2001 / Accepted: 13 June 2001 / Published online: 16 August 2001

Abstract A newly developed spectrometer for energy-dispersive micro X-ray fluorescence spectrometry has been designed for the demands of archaeometry. ArtTAX combines the advantages of non-destructive and sensitive multi-elemental analysis at sub-mm resolution with the possibility of working outside the laboratory. The spectrometer consists of an air-cooled, low-power molybdenum tube, new generation polycapillary X-ray optics, a silicon drift detector without the need for liquid-nitrogen cooling, a CCD camera, and three light diodes for sample positioning. The motor-driven measurement head is fixed on a x,y,z-flexible tripod support which can be assembled and dismantled within minutes. The spot size of the primary X-ray beam was determined to be 94 μm for the Cu(Kα) energy, the detection limits are in a range of a few tens of μg g^{-1} for the medium energy-range in glass. Additional open helium purging in the excitation and detection paths enables the determination of elements down to sodium, thus avoiding vacuum conditions or a size-limiting sample chamber. A selection of qualitative and quantitative results on pigment, metal, glass, and enamel analyses are presented to show the potential of ArtTAX in the field of art and archaeology.

Dedicated to Professor Jörn Müller on the occasion of his 65th birthday.

H. Bronk (✉) · S. Röhrs
Technische Universität Berlin,
Institut für Anorganische und Analytische Chemie,
Sekretariat C2, Strasse des 17. Juni 135, 10623 Berlin, Germany
e-mail: bronoecc@mailszrz.zrz.tu-berlin.de

A. Bjeoumikhov · N. Langhoff · J. Schmalz · R. Wedell
IfG-Institut für Gerätebau GmbH,
Rudower Chaussee 29/31, 12489 Berlin, Germany

H.-E. Gorny · A. Herold · U. Waldschläger
INTAX GmbH Berlin,
Schwarzschildstr. 10, 12489 Berlin, Germany

Introduction

In archaeometry, especially for the analysis of unique and valuable objects, the analytical technique should be able to deliver as detailed information on the material's composition and/or structure as possible without causing any damage to, or even changing, the artifact. In practice a compromise must be found between these two extreme requirements which – at least at present – can never both be satisfactorily fulfilled at the same time.

The archaeometric scientist has a range of powerful non-destructive techniques at hand, however, for example X-ray fluorescence (XRF) or proton-induced X-ray emission (PIXE) (to name only two established methods for quantitative inorganic elemental determinations). An impressive selection of XRF applications on a variety of historical materials was recently given in a special issue on the cultural heritage of X-ray spectrometry [1]. The use of PIXE in the field of art has been reviewed by Johansson and Campbell [2] and by Demortier and Adriaens [3].

Many of these devices have major drawbacks, which sometimes limit their range of application. For example, much of the equipment is stationary, i.e. it requires transport of the objects into the laboratory. Occasionally this involves unacceptable risk; sometimes, e.g. for frescos, it might be impossible. Portable XRF spectrometers are commercially available; they are primarily used for geochemical or metallurgical surveys but have also been applied, e.g., to archaeological rock samples [4]. These spectrometers are usually equipped with a radionuclide source and, because of their low X-ray intensities, are restricted to large spot sizes (usually more than 1 cm in diameter) of the incident beam. Lateral resolution is a crucial factor in the investigation of filigree objects, painting details, or inhomogeneities and is, therefore, ideally in the mm or even sub-mm range.

In conventional XRF the sample chamber is usually part of the spectrometer and vacuum conditions are used for determination of elements between Z=11 and 19 (Na to K). This is unsatisfactory art analysis for two reasons –

a sample chamber means severe limitation of object size and shape and working under vacuum (as essential, e.g., for glasses) means unpredictable risk for fragile pieces.

The μ-XRF spectrometer introduced here is an attempt to overcome these limitations and was especially designed to meet the demands of archaeometry. This was made possible by substantial technological developments in recent years especially in the field of X-ray focusing optics [5] and the development of silicon drift chamber (SDD) detectors without the need for liquid nitrogen cooling [6]. The first use of a portable energy-dispersive XRF instrument with SDD detectors in the field of archaeometry was reported by Fiorini and Longoni [7] and Moioli [8]. In an earlier publication by Cesareo et al. [9] the use of other non-cryogenic X-ray detectors in portable systems for archaeometry was described. A review of portable systems for energy-dispersive XRF was given by Cesareo et al. [10]; this also covers application to various art objects, e.g. gold and bronze objects and paintings. Janssens and Adams [11] have summarized applications of μ-XRF (i.e. with micrometer resolution) using laboratory and synchrotron facilities. A new portable μ-XRF was introduced by Bichlmeier [12] – measurements on medieval gold artifacts and Merovingian glass pearls were performed in air with a rhodium tube and a polycapillary optics providing a spot size of 140 μm.

ArtTAX has been constructed within an ongoing research project, that started in April 1999, on the problems of dating Limoges painted enamels [13]. It is distinguished by a comparatively inexpensive and flexible open set-up which enables investigation of almost any object without even touching it. The spectrometer can be easily installed in a museum store, a church, or a restorer's room for external use. We trust that this μ-XRF spectrometer will considerably increase the number and nature of art and archaeological objects now accessible to scientific examination and will, therefore, contribute to our knowledge of the past.

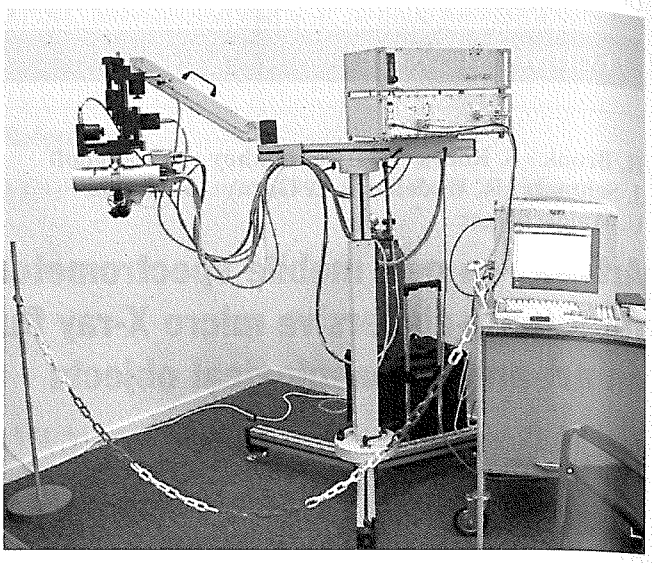

Fig. 1 The mobile μ-XRF spectrometer ArtTAX, complete set-up

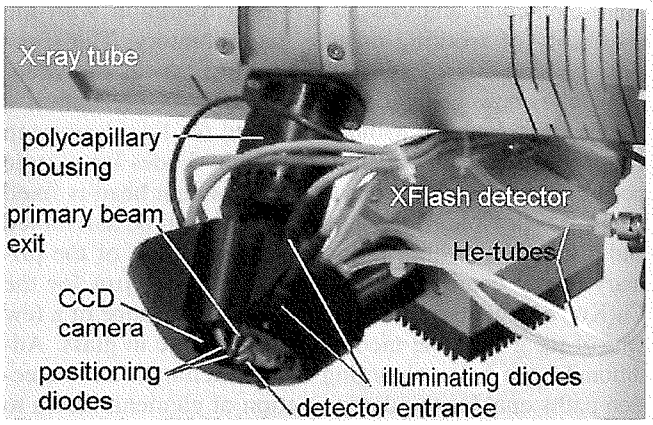

Fig. 2 The ArtTAX spectrometer head (size approx. 32 cm×20 cm)

Spectrometer set-up ArtTAX – technical details

The design of the ArtTAX measuring head, comprising an X-ray source for excitation, a new-generation focusing polycapillary lens, an X-ray detector, a CCD camera, and a helium gas purging system, is also optimized for acquisition of multielement spectra inside the concave parts of objects. The portable system is shown in Figs 1 and 2 and its components are described below.

X-ray source and detection system

A low-power metal–ceramic-type MCBM 50 X-ray tube [14] with molybdenum target is used as excitation source. With an anode spot size of 70 μm×50 μm, a high voltage of 50 kV and a maximum power of 30 W is possible. The radiation-protecting tube housing is equipped with an electrical shutter and safety functions, externally controlled by a PC. A free surveyor determined the scattered radiation from primary beam with maximum power. The beam was set vertically downwards and was scattered by a 1 L water PE bottle. At a distance of 1 m only 0.5 mS h^{-1} were detected. For additional irradiation protection the operator is placed behind a mobile wall with 0.5 mm Pb equivalent.

The X-ray fluorescence is detected by means of an electro-thermally cooled XFlash detector (Röntec, Berlin, Germany), which is a silicon drift detector with high-speed, low-noise electronics. Typical energy resolution for Mn-Kα radiation at a count rate of 10 kcps is 160 eV. The detector has an active area of 5 mm^2 and an 8 μm-thick Dura-beryllium window.

The geometry between primary beam, sample, and detector is fixed at 0°/40° relative to the perpendicular of the sample surface.

Polycapillary optics

The polycapillary lens is an important part of the ArtTAX measuring head because it realizes a microspot of primary X-radiation of high intensity on the sample surface if the design of the capillary system and adjustment of the X-ray tube are optimized. Polycapillary systems are an ensemble of glass capillaries which form a united monolithic structure with a complicated shape [15, 16, 17]. Each capillary transports radiation by means of multiple total external reflections on its inner surface. A system of bent capillaries, which at one end are pointed at the source and at the other end at a chosen point, therefore focuses the radiation from one point to another. Because each capillary captures only radiation within a defined angular interval, which is approximately twice the critical angle of total external reflection, the optimum values for the anode spot and the focal spot size are given by the formula:

$$S_{s,f} = \left(d^2 + \left(f_{s,f}\Phi_C\right)^2\right)^{1/2} \quad (1)$$

where $S_{s,f}$ is the size of the source or the focus, $f_{s,f}$ are the focal distances from the source or the focus, respectively, d is the inner diameter of the capillary channels, and Φ_C is the critical angle for total external reflection for the radiation used and the glass material.

The optimum size of the source and the size of the focal spot thus depend on the radiation energy and the focal distances at the entrance and exit of the system. Varying the general size of the capillary lens and considering the proportions indicated above it becomes possible to vary the source and focal spot sizes within a large interval from 10 µm to several millimeters. A capillary lens optimized for a source 50–100 µm in size, which focuses the radiation on a focal spot of the same order of magnitude, is called "full mini-lens".

Figure 3 schematically depicts such a mini-lens, which is used for the ArtTAX spectrometer. The sizes of the individual channels at the entrance and exit are approximately 2 µm. In the middle of the capillary these channels are widened to 3 µm. Geometrical data for the mini-lens are presented in Table 1. Spot sizes and intensity gains compared with the same set-up geometry, without capillaries, in two typical energy ranges, are presented in Table 2. The beam sizes at 7–9 keV and at 16–19 keV are 100 µm and 75 µm, respectively.

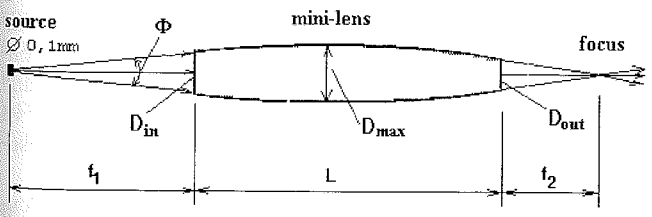

Fig. 3 Schematic diagram of the polycapillary lens No. 02mls02

Table 1 Geometric data for the polycapillary lens No. 02mls02

f_1, mm	37.0±1
f_2, mm	29.5±0.1
L, mm	62.5
D_{in}(structure/cover), mm	3.5/4.7
D_{out} (structure/cover), mm	3.8/4.9
D_{max}(structure/cover), mm	5.6/7.7
Φ, rad	0.1
$R=f_1+f_2+L$, mm	129.0±1

Table 2 Physical properties of the mini-lens No. 02mls02

E, keV	8.0–9.0	16.0–19.0
Focus size[a], µm	100	75
Intensity gain[b]	2090	1120

[a]FWHM, scanning by a 15 µm pinhole
[b]Intensity gain=Intensity through a 15 µm pinhole at lens focus/ Intensity of the direct beam through a 15 µm pinhole

Figure 4 shows two spectra obtained from the transmitted beam, one measured in the focal plane of the lens and the other as the direct beam at the same distance from the source without a capillary. For this test a micro-focus X-ray tube with a Cu anode at U=26 kV and I=18 µA was used. The source spot was 0.1 mm in diameter. The X-radiation was measured by means of the X-Flash detector with an absorber of 0.1 mm Cu and 0.2 mm Al.

Imaging system and sample positioning

An integrated CCD camera gives an image of the sample region under investigation (8 mm×8 mm). Two dimmable white LEDs illuminate the sample from different angles to optimize the image quality and contrast depending on the sample type and surface.

The exact position of the beam on the sample and the exact distance between object and spectrometer is controlled via three beam-crossing diodes. Their point of intersection is adjusted to the focus of the mini-lens and is visualized by the camera.

A portable stand manufactured by TSO (Pulsnitz, Germany) is used to position the measuring system relative to the object under investigation. This stand is characterized by stable construction (weight ca. 50 kg) and high stability. Its different parts can easily be adjusted. The setting interval of the stand and the variable measuring head suspension enable a large positioning interval. The working height lies between 0.5 m and 1.5 m.

The measuring head ArtTAX and a motor-driven x,y,z positioning stage, which consists of three equal modules with a maximum travel of 50 mm in each direction, can be directly mounted on the vibration-damped swivel arm of the support's cantilever. Reproducibility of measurement position of ±10 µm is guaranteed.

The suspension for the measuring head enables to rotate it continuously around a maximum angle of –10° and 90° and to fix it at a definite angle depending on the slope of the studied surface.

As the electronic unit of the device is mounted on the stand cantilever and a 10-L helium bottle can be clamped

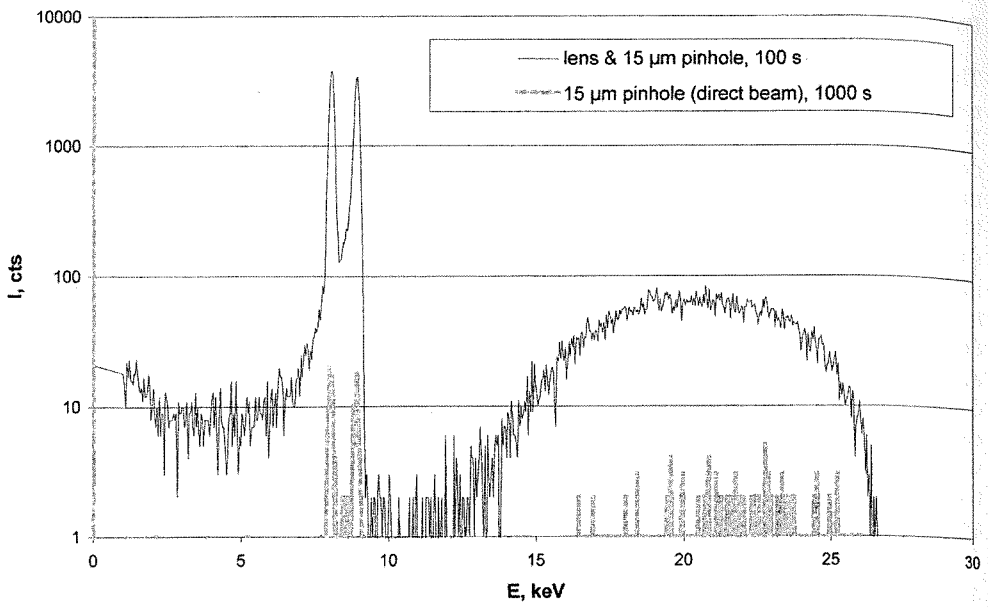

Fig. 4 X-ray spectra measured by means of: *gray* – a 15 µm pinhole at a distance of 129 mm from the source (measurement time 1000 s); *black* – a 15 µm pinhole in the focus of the lens (measurement time 100 s)

to the stand by means of a special fixture, the complete ArtTAX system can easily be moved between different objects of investigation.

Assembly and dismantling of the complete set-up can be achieved within approx. 30 min. The whole equipment, which is transportable by means of a utility car, consists of three boxes and an industrial PC (total weight ca. 100 kg), and a 10-L helium bottle if required.

Control and data-handling software

All essential hardware functions, e.g. X-ray source condition settings and generator safety functions, the start/stop of measurements, real time and live time XRF spectra accumulation and storage, visualization of spectra on the PC screen, and x,y,z-positioning by use of stepper motors are controlled via a serial interface by an industrial PC with the Windows-based ArtTAX-Ctrl software (Intax, Berlin, Germany). Energy and FWHM calibration, element identification, background calculation, peak fitting, peak and background net area calculation, and report functions are the main features for qualitative analysis. A data and spectra export function delivers the required .spe files for quantitative analysis with the AXIL/QXAS software package from the IAEA (International Atomic Energy Agency, Seibersdorf, Austria). The QXAS applies a direct comparison method of count rates or an elemental sensitivity method (considering absorption effects), both using standard sample sets with similar element concentrations, or alternatively a standardless fundamental parameter calculation.

Spectrometrical characterization

Spot-size measurement

The lateral resolution of a mobile device might be expected to be not as good as for stationary equipment, owing to unavoidable vibrations of the measurement head after movement of the x,y,z-stage and slight shaking of the floor. It was, therefore, experimentally important to determine the "true" spot size of the ArtTAX mini-lens as a sum of the physical spot size of the polycapillary and an additional mechanical "vibration" part.

Spot-size measurement was conducted by performing a line scan over a sharp copper–gold edge in 10-µm steps. The measurement conditions were 40 kV, 0.6 mA, 60 s lifetime, helium atmosphere.

The net fluorescence intensity of the Cu(Kα) line at 8.047 keV and the Au(Mα1) line at 2.123 keV were evaluated. The decrease and increase of fluorescence intensity, respectively, were fitted according to a Boltzmann function. The full width at half maximum (FWHM) of its first derivative was taken as the value for the lateral resolution at this energy value (Fig. 5).

For the Cu(K) energy a spot size of 94 µm was calculated. In good agreement with theoretical considerations of the total reflection within a glass capillary, the value for the lower-energetic Au(M) line was found to be slightly reduced in lateral resolution – the value was 108 µm. The experiment also showed that the "true" lateral resolution of the ArtTAX spectrometer was not significantly worse than for mechanically fixed stationary arrangements (for comparison see Table 2).

It must be emphasized that our first practical experience demonstrated the superiority of the lateral resolution available with this equipment compared with a normal pin-hole design (the spot size limited to a minimum of ca.

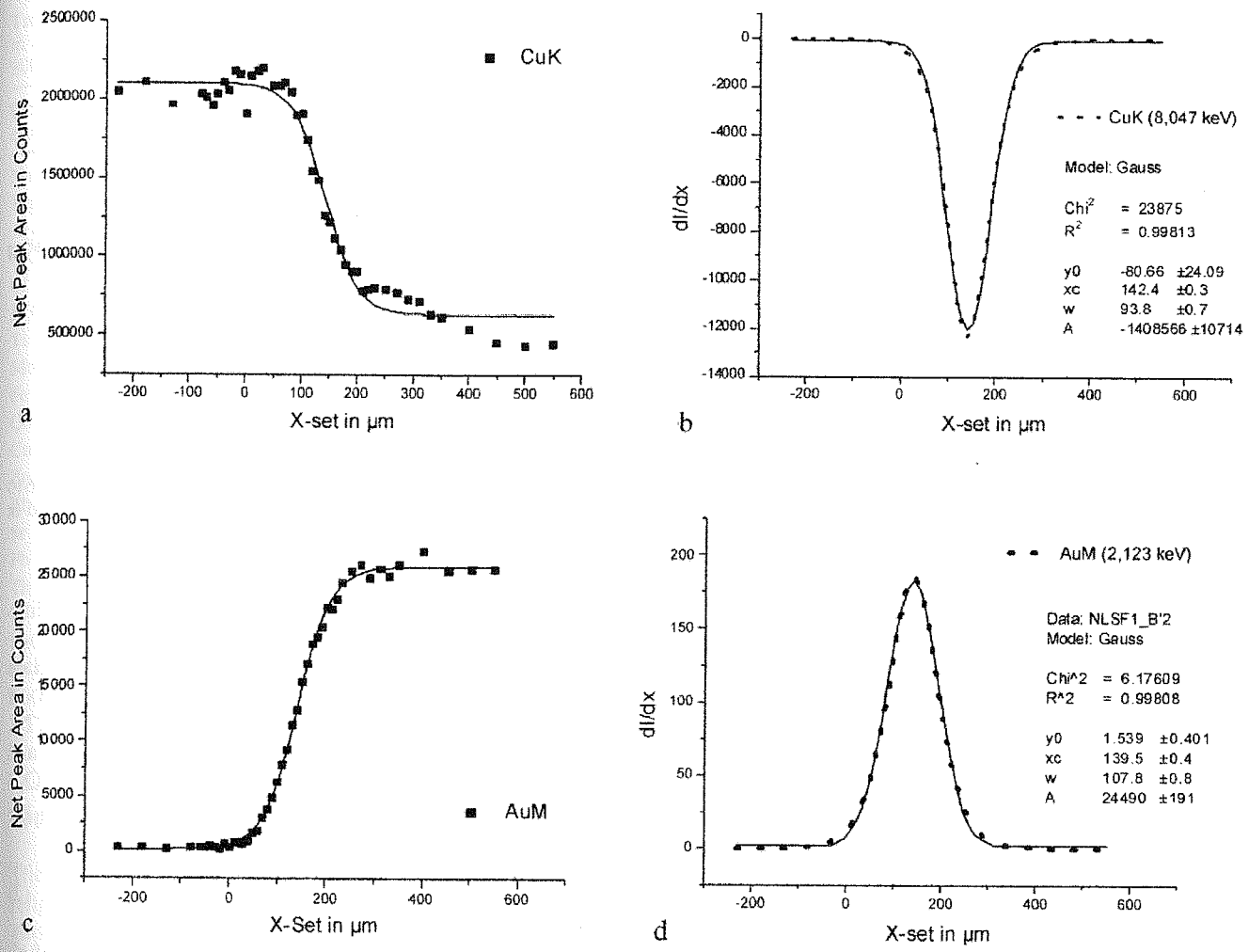

Fig. 5 Spot-size calculation of the polycapillary optics for the Cu(Kα) (**a**, **b**) and Au(Mα) (**c**, **d**) lines. Measurement conditions: 40 kV, 600 µA, 60 s lifetime, 0.8 L min^{-1} He

0.5 mm) especially for investigation of painting details and filigree objects such as jewelry. We also assume that a smaller beam size – ca. 30 µm has so far been achieved in laboratory facilities – is difficult to realize in a mobile device and, it seems to us, is not necessary for most applications in archaeometry.

Repeatability of positioning

The exact positioning of the distance between sample and spectrometer (designated as the z parameter) is crucial to the accuracy and precision of quantitative investigations. The repeatability with and without re-positioning of the spectrometer head via the camera image was, therefore, compared for the Ca(Kα) main line of a standard glass (Corning D). The net count rate was approx. 360 cps. Without moving the spectrometer head between the individual measurements, a repeatability of 0.7% (n=20), expressed as relative standard deviation RSD of the net peak area, was calculated. This value is determined by the tube and detector stability and the statistical counting error. For comparison with this, a second experiment was performed with a new optical adjustment of the z axis for every single measurement. It was observed that the sample distance could be set with an accuracy of ±0.1 mm for even, unpolished surfaces. Within this limit the spot size does not increase significantly. Repeatability with re-positioning was determined, for the same element line and the same conditions, to be 0.9% RSD. Repeatability is, therefore, reduced only minimally by re-positioning. This situation might become more difficult for highly reflective or polished sample surfaces, because the true position of the diode spots is not easy to recognize. In such circumstances attachment of a small piece of a thin tissue (ca. 0.1 mm thick) to the object with a drop of ethanol, or any other convenient liquid, is recommended. The dried tissue can easily be removed after adjustment; the sample distance must then be corrected for the tissue thickness.

Helium purging

Fluorescence lines below 3.5 keV are significantly absorbed in an air-filled path of 10 mm between sample and detector. To give an example, the sodium fluorescence has

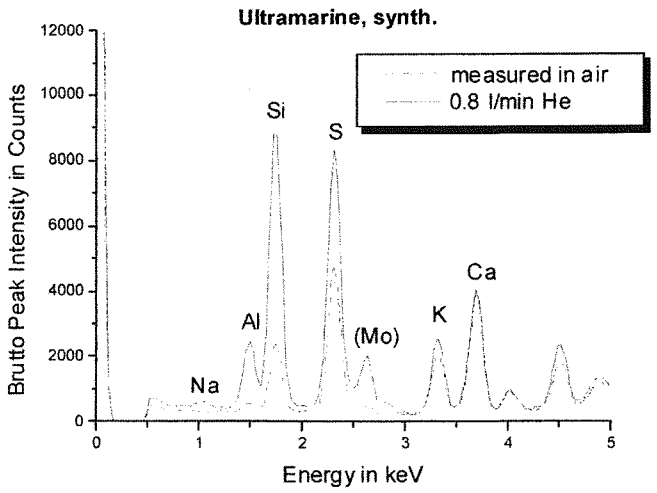

Fig. 6 Spectra obtained an ultramarine pigment with and without helium purging (cut-out). Measurement conditions 40 kV, 600 µA, 300 s lifetime

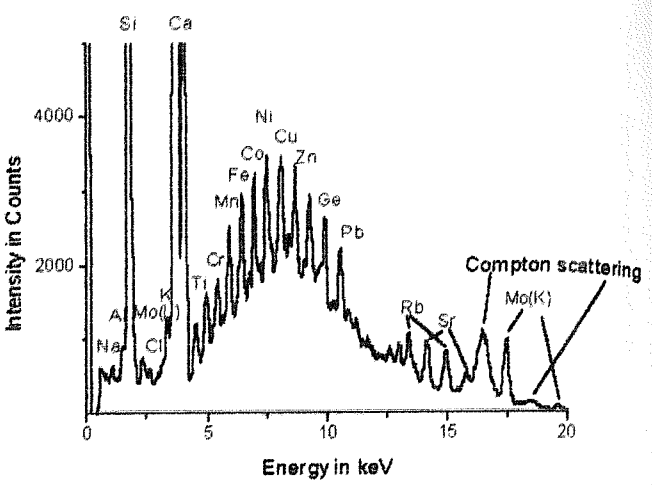

Fig. 7 Spectrum obtained from the reference glass NIST 610 (500 µg g^{-1} trace element standard). Measurement performed at 40 kV, 600 µA, 300 s, 0.8 L min^{-1} He

a transmission of only 1.9% under such conditions whereas in a helium atmosphere transmission is still 98.5%. Vacuum conditions (not an option for the spectrometer presented here) or, alternatively, purging with helium are, therefore, necessary for the determination of elements with Z<20 (Ca).

For the feasibility of non-touching investigations and for better sample observation it was desirable to maintain an open arrangement for helium purging.

All excitation and detection paths can be rinsed with inert gas which is directed, by use of two gas jets, towards the sample surface. The polycapillary, also, has been filled with helium and shut with two beryllium windows 25 µm thick. This leads to a considerable increase of the Mo(L) excitation intensity and improved detection limits for the light elements.

A total helium flow of 0.8 L min^{-1} was found to give optimum signals. Comparison of open geometry with an arrangement with an additional plastic collar revealed no differences between fluorescence intensities. Helium of low purity (so called "balloon gas") is sufficient for purging and helps to reduce costs.

Figure 6 depicts the effect of the helium atmosphere. The spectra of a synthetic ultramarine pigment – a sodium aluminum silicate with enclosed sulfur radicals – clearly shows the strong absorption of the X-ray fluorescence by air at energies lower than 3.5 keV (Na–K).

The repeatability of the determination of sodium in a soda-lime reference glass with 14.3% Na_2O (Corning A) was determined to be 7.0% RSD (n=15, no re-positioning).

Detection limits

Detection limits (DL) were calculated for a series of lead-free standard glasses. The actual measurement conditions were 40 kV (45 kV for Sn, Sb and Ba), 600 µA, 300 s lifetime, 0.8 L min^{-1} He.

A spectrum obtained from a certified standard glass (NIST 610) with an approximate weight fraction of 500 µg g^{-1} of various trace elements (e.g. Mn, Fe, Cu, Ni, Co, Pb, Rb, Sr, etc.) is shown in Fig. 7. (The sodium and aluminum content are approx. 14% Na_2O and 2% Al_2O_3.)

The detection limits were calculated as 3σ values according to Eq. (2):

$$DL = 3\sqrt{BG}\,\frac{w_i}{N_{i,netto}} \qquad (2)$$

where BG is the background, w_i the weight fraction of element i, and $N_{i,Netto}$ the net peak area of element i.

DL for 20 elements are listed in Table 3.

When molybdenum was used as tube target material, and with the highest intensity gains of the polycapillary at approximately 8–9 keV, best detection limits were achieved for a medium energy range of ca. 5–15 keV. Detection limits for the chosen measurements conditions (i.e. with a moderate accumulation time) were between 18 and 120 µg g^{-1}. For higher energies above the Mo(K) excitation energy the sensitivity is necessarily reduced, also because of poorer detector efficiency for the SDD detector, although elements such as tin and antimony in glass can still be detected above mass fractions of approximately 0.03 to 0.05% of the oxides, via their K-lines, even for BaO the detection limit is below 0.5%. The detection limits achieved for the energy range between 1 and 3 keV by purging with helium can be considered as satisfactory for investigation of pigments, precious stones, and, especially, glass and enamel (which is here regarded as glass on metal). Although detection limits for Na_2O, Al_2O_3, and MgO – ca. 4%, 2%, and 0.4%, respectively – are not as good as for most conventional XRF systems with larger spot sizes and a vacuum chamber, they are a considerable improvement compared to measurements in air, and easily enable classification of different types of glass.

Table 3 Detection limits (DL) for different elements (3σ values) in lead-free glass. Measurement conditions: 40 or 45 kV, 600 μA, 300 s lifetime, 0.8 L min^{-1} He

Element or element oxide	Fluorescence series	DL in wt% or μg g^{-1}
Na_2O	Na(Kα)	3.8%
MgO	Mg(Kα)	2.0%
Al_2O_3	Al(Kα)	0.39%
P_2O_5	P(Kα)	0.34%
Cl	Cl(Kα)	0.022%
K_2O	K(Kα)	49 μg g^{-1}
Ti	Ti(Kα)	27 μg g^{-1}
Mn	Mn(Kα)	22 μg g^{-1}
Fe	Fe(Kα)	19 μg g^{-1}
Co	Co(Kα)	18 μg g^{-1}
Cu	Cu(Kα)	19 μg g^{-1}
Zn	Zn(Kα)	22 μg g^{-1}
Rb	Rb(Kα)	46 μg g^{-1}
Sr	Sr(Kα)	29 μg g^{-1}
Pb	Pb(Lα)	29 μg g^{-1}
Th	Th(Lα)	106 μg g^{-1}
U	U(Lα)	120 μg g^{-1}
SnO_2	Sn(Kα)	0.032%
Sb_2O_3	Sb(Kα)	0.052%
BaO	Ba(Kα)	0.44%

Applications

The μ-XRF is capable of quantitative analysis of a wide range of object made of different materials, i.e. metals, glass, ceramics, gemstones, and different pigments on paintings, frescos, illuminated manuscripts etc.

An application of a first ArtTAX prototype (still without X-ray optics and helium purging) – the non-destructive characterization of historical iron gallus inks – was published by Hahn [18].

Metals

The feasibility of investigation of metals is briefly illustrated by investigation of the so-called "Sceptre of Charles the Great" (Kunstgewerbemuseum Berlin). The sceptre, length approximately 50 cm, is dated as 15th century and is made of agate and gold mountings.

μ-XRF measurement in the museum revealed that the mountings are made not of massive gold but of a gilded silver alloy. The small beam size enabled separate investigation of the golden surface and of small damaged areas – increased signals from silver and copper and a lower signal for gold were obtained from the latter. Quantification of the gold layer and the bulk alloy was not easily feasible because the information depth of the XRF was larger than the thickness of the gilding layer.

The presence of mercury in the gold surface proved use of the technique of "fire gilding" for this medieval piece (Fig. 8). Fire gilding is a technique in which a mixture of gold and mercury was applied and the object subsequently heated to volatilize the mercury [19].

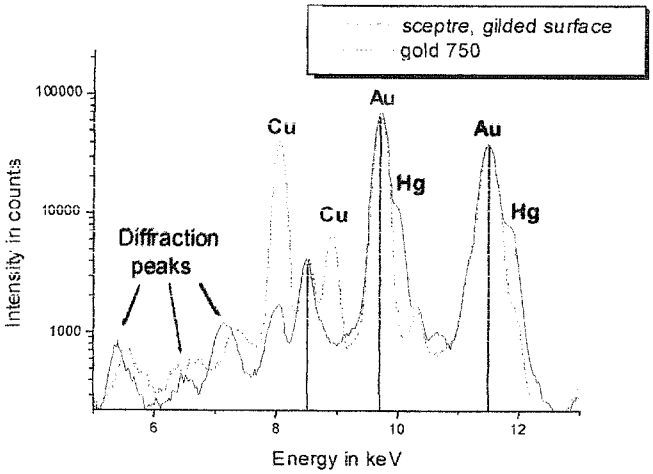

Fig. 8 Spectrum cut-out obtained from the gilded surface of the so-called "sceptre of Charles the Great". Comparison was made with a 750 jewelry gold to illustrate the presence of mercury

A particular feature of materials with a crystalline structure in the μ-XRF is also evident from Fig. 8. The strong focusing of a high-intensity primary beam leads to additional diffraction peaks (in this example between 5 and 6 keV) for energy values which fulfil the Bragg rule at the given geometry.

Glass and enamel

Initial quantitative calculations using standard glasses of similar composition were performed using the elemental sensitivity method provided by the QXAS software package. Peak deconvolution was performed by use of AXIL. For verification the results obtained were compared with those from electron probe microanalysis (EPMA), a well-established analytical technique for the investigation of historical glasses. EPMA requires a small sample – ca. 1 mm^3. This is embedded in epoxy resin, ground, polished, and carbon-coated for analysis. The EPMA reference measurements were conducted with an ARL-microprobe (SEMQ) instrument equipped with an energy-dispersive spectrometer (KEVEX-WINEDS) with an Si(Li) detection system with a thin polymer window for light-element detection. The conditions were chosen to ensure that no migration of Na^+ and/or K^+ occurred during measurement, by working with the smallest possible irradiating electron current and a moving beam. Operation and theoretical background have been described in detail in the literature [20]. The accuracy of EPMA is approximately 1–2% rel. for main elements and can be up to 15–20% for elements near the detection limit (approx. 0.2% of the oxide in glass).

Results from two single μ-XRF measurements without further sample treatment were compared with those obtained by use of energy-dispersive EPMA for a 18th century mirror glass from the "Merseburger Spiegelkabinett"

Table 4 Quantitative results from μ-XRF and EPMA analysis of a 18th century mirror glass

	μ-XRF			EPMA (n=2)
	Measurement 1	Measurement 2	Average	
Na_2O	<DL	<DL	<3.8	4.65
MgO	<DL	<DL	<2.0	<0.2%
Al_2O_3	2.17	2.30	2.23	2.15
SiO_2	63.5	64.6	64.0	63.0
P_2O_5	<DL	<DL	<0.34	<0.2
K_2O	17.6	17.9	17.8	18.5
CaO	9.59	9.79	9.69	9.84
TiO_2	0.085	0.086	0.085	0.12
MnO	0.41	0.42	0.41	0.36
Fe_2O_3	0.22	0.23	0.22	0.22
SrO	0.041	0.041	0.041	<0.2
BaO	<DL	<DL	<0.44	<0.2

All data are given in wt%
μ-XRF values are not normalized
DL=detection limit

(Kunstgewerbemuseum Berlin) [21]. The results are compared in Table 4. The measurement conditions for μ-XRF were 45 kV, 600 μA, 100 s lifetime, and 0.8 L min^{-1} He.

The results of the two methods are in good agreement. The relative differences found for the main and minor elements are between 1.5 and 3.7% relative and can therefore be regarded as satisfactory for many archaeometric problems. For element oxide contents below 0.5% the difference is larger (e.g. for MnO and TiO_2 14% rel.) but still within the normal range of precision of the SEM. Na_2O was not found by μ-XRF – probably because of a common effect in XRF analysis of historical glasses, for which values for this element are often too low. It is well-established that strong depletion of sodium oxide is observed in corrosion layers on glass. The information depth of the sodium fluorescence signal is approximately 1–2 μm and is, therefore, severely affected by deterioration processes (even if they are not yet visible). To obtain accurate results local polishing of the area of measurement would have been necessary.

In a first measurement campaign at the Kunstgewerbemuseum Berlin the mobile μ-XRF spectrometer ArtTAX was used for non-destructive investigation of painted enamels from the French city Limoges. This highly sophisticated art of painting with glass pastes and firing them on a copper carrier had its peak in the late 15th to early 17th centuries. Recent art-historical research cast doubt on the authenticity of some of the Limoges painted enamels in the collection of the Kunstgewerbemuseum [22]. During the second half of the 19th century – a time which saw a revived interest in the art of the Medieval ages and the Renaissance – an unknown number of replicas and deliberate forgeries of painted enamels in the Limoges School style were made.

The minute execution of painting details in different colors and materials made lateral resolution of approxi-

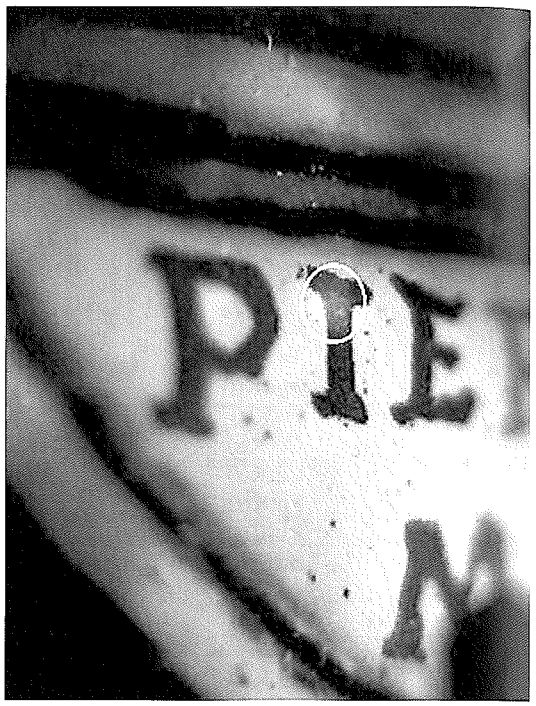

Fig. 9 Detail of an artist's signature on a 16th c. Limoges painted enamel (line thickness app. 150 μm). The ellipse represents the area lit by the overlaid red positioning diode spots

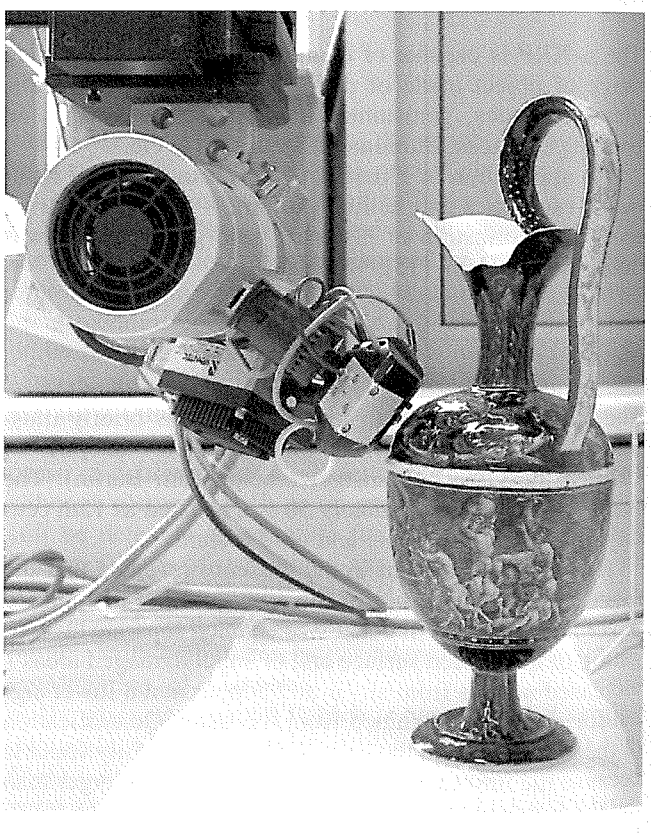

Fig. 10 μ-XRF investigation of a Limoges painted enamel (jug dated "1564" with bacchus procession) in the Kunstgewerbemuseum Berlin

Fig. 11 S
bacchus p
saille); (**b**
from light

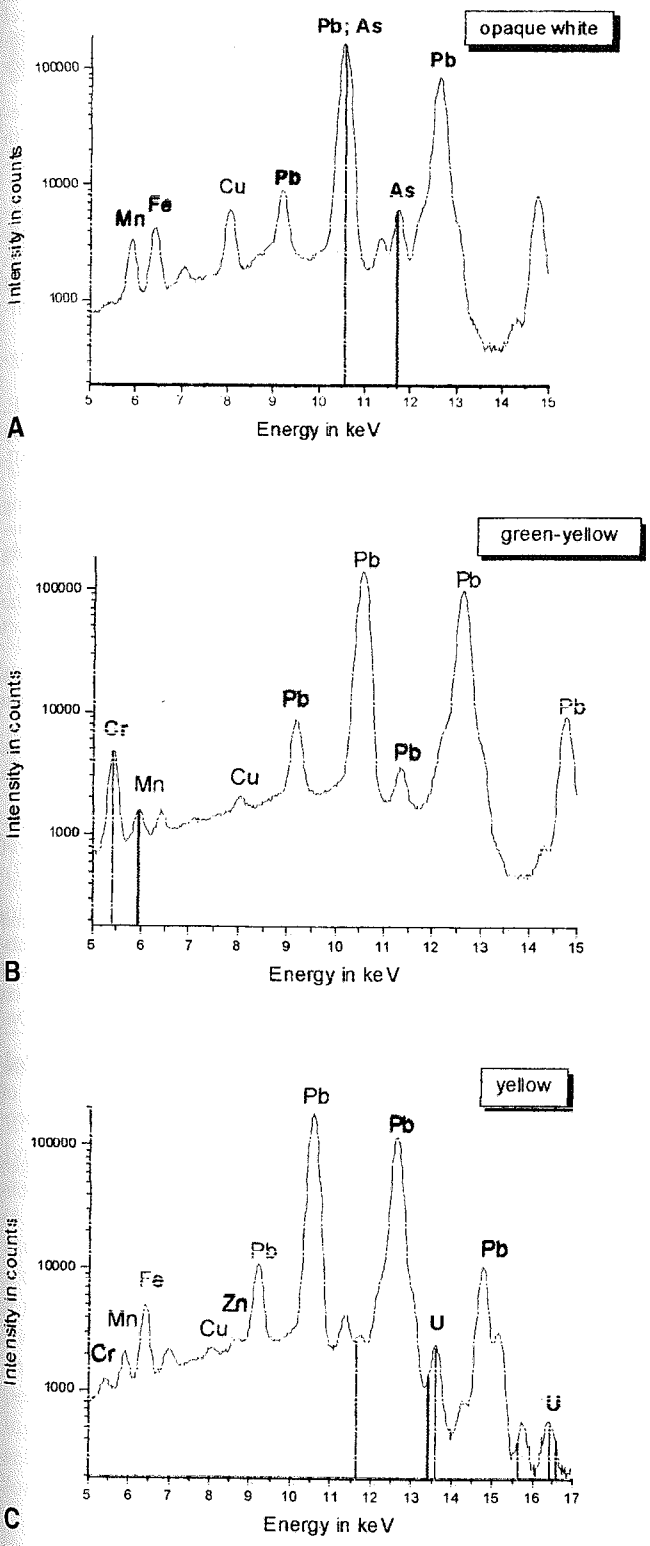

Fig. 11 Spectra obtained from the polychrome enameled jug with bacchus procession: (**a**) spectrum from opaque white enamel (grisaille); (**b**) spectrum from transparent green enamel; (**c**) spectrum from light yellow enamel

mately 100 µm essential. Figure 9 illustrates a detail from a signature with a line thickness of app. 150 µm which could be analyzed separately from the opaque white background.

The results from µ-XRF measurements of a polychrome jug dated "1564" showing a triumphal procession of bacchus (Fig. 10) are a good example of the power of the new device. The measurements (Fig. 11) identified lead arsenate as opacifier in opaque white areas, in contradiction to 16th century enamels which contain tin oxide in a lead-rich matrix. An enamel with a green-yellow tint contained chromium, which is a dating marker for the 19th century. Furthermore, in transparent yellowish enamel from this piece the element uranium was detected in significant amounts; this element was introduced into glass and enamel production only in the eighteen-thirties [23, 24].

Even with these readily available qualitative results a 16th century date can be definitely excluded, which is in agreement with the art-historical research on this jug.

A few known limitations of µ-XRF in the field of archaeometry should, however, be mentioned.

The area to be analyzed must be chosen carefully with regard to possible inhomogeneities or surface compositional change, as a result of deterioration, because these might have a serious influence on the analytical results. Furthermore, similarly to conventional XRF, the information depths for different elements and materials is high (in the micron to even millimeter range). The quantification of layered materials might, therefore, be not always possible. Also sample surface roughness or small particle size (e.g. chips) can cause quantification problems as a result of geometric effects. The influence of particle size on fluorescence intensities was shown by Rödel [25].

It should also be emphasized that special care must be taken with materials sensitive to ionizing radiation (i.e. non-conducting materials such as glass or certain pigments). We found that even irradiation times of only 5 min (at 45 kV, 600 µA) can occasionally cause weak brown discoloration of white enamels, porcelain, or transparent glass. This effect, explained by the formation of so-called "color centers" [26], is partly reversible with time but should be carefully taken into account when choosing spectrum accumulation times.

Conclusion

Mobile energy-dispersive µ-XRF spectrometry enables a wide range of new applications in the field of art and archaeology. It will be possible to perform material investigations on many more objects for which scientific analysis has not hitherto been feasible. The new ArtTAX spectrometer described here combines the general advantages of XRF, such as non-destructivity, satisfactory detection limits, and fast multielemental analyses with excellent lateral resolution, mobility, and an open, chamber-less design. For non-deteriorated objects no further sample preparation is required. ArtTAX is commercially available in customer-specified modifications.

More experience must, however, be gained, especially with regard to the sturdiness of the spectrometer in long-term and in-field use. A future focus should be improvement of quantification routines – it is hoped that, especially, the physical models for a standardless quantification using fundamental parameter models will be adapted taking the changed polychromatic and broad-filtered excitation characteristics of capillary optics into account. Without doubt, the technology of capillary fabrication and non-cryogenic detectors will also be the subject of further developments.

Acknowledgements We gratefully acknowledge the generous financial support provided by the German Federal Ministry for Research and Education (BMBF) within the framework "New technologies in the Human sciences" (Grant-No. 03MU9TUB1). We would like to thank the members of the staff at the Kunstgewerbemuseum Berlin, especially Dr Susanne Netzer, for their collaboration and kind permission to perform μ-XRF analysis on various art objects. We are also very grateful to Karin Adam (BAM Berlin) for providing the EPMA analyses.

References

1. Lindgren ES (Guest ed) X-Ray Spectrometry (2000) Special Millennium Issue on Cultural Heritage, Vol 29, No.1
2. Johansson SAE, Campbell JL, Malmqvist KG (1995) Particle-induced X-ray Emission Spectrometry. John Wiley, Chichester
3. Demortier G, Adriaens A (Eds) (2000) Ion Beam Study of Art and Archaeological Objects. Office for Official Publications of the European Communities, Luxembourg
4. Potts PJ, Webb PC, Williams-Thorpe O (1997) J Anal At Spectrom 12:769
5. Janssens KHA, Adams FCV, Rindby A Eds (2000) Microscopic X-ray Fluorescence Analysis. John Wiley
6. Fiorini C, Kemmer J, Lechner P et al. (1997) Rev Sci Instrum 68(6):2461–2465
7. Fiorini C, Longoni A (1998) Rev Sci Instrum 69(3):1523–1528
8. Moioli P, Seccaroni C (2000) X-ray Spectrom 29:48–52
9. Cesareo R, Gigante GE, Canegallo P, Castellano A, Iwanczyk JS, Dabrowski A (1996) Nucl Instrum Methods Phys Res A 380:440–445
10. Cesareo R, Gigante GE, Castellano A, Iwanczyk JS (2001) Portable Systems for Energy-dispersive X-ray Fluorescence. In: Encyclopedia for Analytical Chemistry. Meyers RA (Ed.) John Wiley and Sons, 13327–13338
11. Janssens K, Adams F (2000) Microscopic X-ray Fluorescence Analysis. John Wiley 291–314
12. Bichlmeier S, Hoffmann P, Ortner HM (2000) Anwendung einer ortsauflösenden Röntgenfluoreszenzsonde (Mikro-RFA) zur Klärung kulturhistorischer Fragestellungen. Anwendertreffen Röntgenfluoreszenz- und Funkenemissionsspektrometrie Dortmund 13./14.3.2000, pp 166–174
13. Bronk H, Müller J, Netzer S, Walz A, Baratte S, Tait H, Speel E, Langhoff N et al., Biron I, Adam K et al. (1999) Symp Material Investigations of Limoges Painted Enamels, Berliner Beiträge zur Archäometrie 16:117–181
14. Windeck C, Warrikhoff H. (1998) A New Series of Metal–Ceramic X-ray Tubes for Low-power Applications. Poster, 7th European Conf Non Destructive Testing (ECNDT), Copenhagen, Denmark, May 1998 (www.rtwxray.de/mcb-post)
15. Kanngießer B, Beckhoff B, Malzer W, Arkadiev VA, Bzhaumikhov AA, Gorny H-E (1998) Comparison of Various X-ray Optics for Energy-dispersive X-ray Fluorescence Analysis with X-ray Tubes. Adv X-Ray Anal Vol 40, Proc 45th Annu Conf Applications of X-Ray Analysis, International Centre for Diffraction Data, Pennsylvania, US 1997
16. Arkadiev V, Beloglazov V, Bjeoumikhov A, Gorny H-E, Langhoff N, Wedell R (2000) Surface Vol 1:48–54
17. Langhoff N, Arkadiev VA, Bjeoumikhov AA, Gorny H-E, Schmalz J, Wedell R (1999) Concepts for a Portable X-ray Spectrometer for Non-destructive Analysis of Works of Art. Berliner Beiträge zur Archäometrie Vol. 16:155–161
18. Hahn O, Gorny H-E (2000) Zerstörungsfreie Charakterisierung historischer Eisengallustinten mittels Röntgenfluoreszenzanalyse. Zeitschrift für Kunsttechnologie und Konservierung 14 Heft 2:384–390
19. Anheuser K (1999) Im Feuer vergoldet. AdR-Schriftenreihe zur Restaurierung und Grabungstechnik Bd. 4, Thesis Stuttgart
20. Autefage F, Fontan F (1985) Bull Mineral 108:293–304
21. Bronk H, Fischer Ch, Mühlbächer E, Unger A (1999) Das Merseburger Spiegelkabinett – Wie sind die Spiegelglasflächen zu restaurieren? Restauro Heft 7/99:506–509
22. Netzer S (1999) Maleremails aus Limoges – Der Bestand des Berliner Kunstgewerbemuseums. Staatliche Museen zu Berlin Preußischer Kulturbesitz and G+H Verlag Berlin
23. Richter R (1994) Between Original and Imitation: Four Technical Studies in Basse-taille Enameling and Re-enameling of the Historicism Period. Bull Cleveland Museum Art 81(7): 223–251
24. Speel E, Bronk H (2001) Enamel Painting: Materials and Recipes in Europe from c. 1500 to c. 1920. Archival and Published Sources with Special Focus on Limoges School Pictorial Work from the Renaissance to the Revival period, and on Overglaze Painting on Enamel from the 17th Century Onwards. Berliner Beiträge zur Archäometrie, in press
25. Roedel TC, Bronk H, Haschke M (2001) Investigation of the Influence of Particle Size on the Quantitative Analysis of Glasses by Energy-dispersive Micro X-ray Fluorescence Spectrometry. X-ray Spectrom (accepted for publication)
26. Witze H-D (1984) Zum Einfluß von Spurenverunreinigungen auf die Verfärbung von bestrahlten Kieselgläsern. Silikattechnik 35 Heft 2:57–58